Proceedings of ISINN-29, JINR, E3-2023-58, Dubna, 2023, p.272 –289

Anisotropy in pre-fission neutron spectra of ^{235}U(n,F)

V. M. Maslov[1]

220025 Minsk, Byelorussia

Angular anisotropy of secondary neutrons evidenced in neutron emission spectra (NES), and prompt fission neutron spectra (PFNS). In case of NES it is due to pre-equilibrium/semi-direct mechanism of emission of first neutron in $(n,nX)^1$ reaction, while in case of PFNS it is due to exclusive spectra of pre-fission neutrons of $(n,xnf)^1$. In ^{239}Pu(n,xnf) and ^{235}U(n,xnf) reactions observed PFNS demonstrate differing response to the emission of first pre-fission neutron in forward and backward semi-spheres with respect to the incident neutrons. Average energies of $(n,nf)^1$ neutrons depend on angle of emission θ with respect to the incident neutron beam. The average prompt fission neutron number, fission cross section, TKE are quite dependent on θ as well. Exclusive spectra of $(n,xnf)^{1,..x}$ neutrons at θ~90^o are consistent with ^{235}U(n,F)(^{235}U(n,xn)) observed cross sections and neutron emission data at E_n~0.01–20 MeV. The correlations of the angular anisotropy of PFNS with the relative contribution of the (n,nf) fission chance to the observed fission cross section and angular anisotropy of neutron emission spectra are ascertained. The exclusive spectra of ^{235}U$(n,xnf)^{1,..x}$, ^{235}U$(n,n\gamma)$ and ^{235}U$(n,xn)^{1,..x}$ reactions are calculated simultaneously with ^{235}U(n,F) and ^{235}U(n,xn) cross sections within Hauser-Feshbach formalism with angular anisotropy of $(n,nX)^1$ neutrons. The ratios of mean PFNS energies $\langle E \rangle$ for forward and backward emission of ^{235}U$(n,xnf)^{1,..x}$ pre-fission neutrons are consistent with measured data.

Fission energy of ^{235}U(n,F) reaction is distributed between fission fragments kinetic energy, their excitation energy and kinetic energy of pre-fission neutrons. Pre-fission neutrons influence the PFNS shape in the energy range of E_n~E_{nnf} – 20 MeV, E_{nnf} being the threshold energy of ^{235}U(n,nf) pre-fission neutrons. They influence also the shape of TKE of fission fragments and products, prompt neutron number, mass distributions and produce the step-like structures in observed fission cross section. Pre-fission neutrons define PFNS shape of ^{235}U(n,F) [1–5] at E_n~E_{nnf} – 20 MeV. The variation of observed average energies $\langle E \rangle$ in the vicinity of ^{235}U(n,xnf) reaction thresholds, as shown in [6–11], are defined by the exclusive spectra of $(n,xnf)^{1,..x}$ neutrons. Henceforth, the upper indices $(1...x)$ notify the emitted pre-fission neutrons. The amplitude of variations of $\langle E \rangle$ in case of ^{235}U(n,F) [7, 9, 10, 12] were confirmed by PFNS measured data ^{235}U(n,F) [4, 5] in E_n~1 – 20 MeV energy range.

Pre-fission neutrons in [1–5] counted in coincidence with fission fragments, without separation with respect to the fragment masses. The evaporation neutrons emitted in a spherically symmetric way with respect to the neutron beam direction. The angular anisotropy of PFNS observed in [1] for ^{239}Pu(n,F), is generally due to pre-equilibrium emission of $(n,nX)^1$ neutrons. Henceforth, the direction of emission of $(n,nX)^1$ neutrons, as well as that of $(n,n\gamma)^1$, $(n,2n)^1$, $(n,3n)^1$ and $(n,nf)^1$, $(n,2nf)^1$ and $(n,3nf)^1$ neutrons, is correlated with the momentum of the incident neutrons. The direction of the neutrons emitted from the fission fragments correlates with the fission axis direction mostly. Both kinds of neutrons counted in coincidence with fission fragments. In [1–5] PFNS detected with ~50 counters mounted around beam direction.

[1]mvm2386@yandex.ru

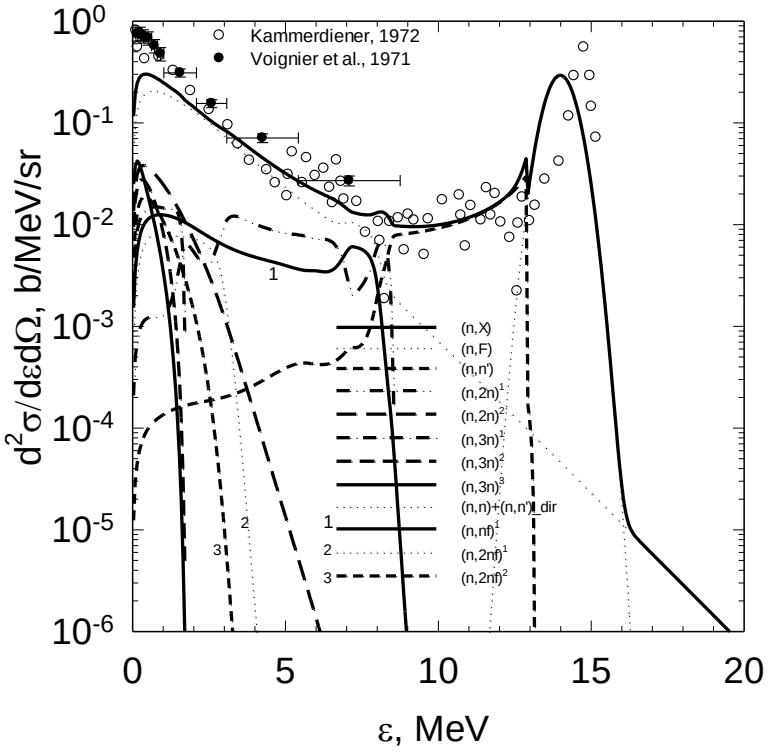

Fig. 1. Double differential neutron emission spectra for ^{235}U(n,F) at E_n =14 MeV, $\theta \approx 30^o$ and its partial contributions; full line – (n,nX); dotted line – (n,F); dashed line – $(n,n\gamma)^1$; dash double dotted line –$(n,2n)^1$; dashed line–$(n,2n)^2$; dash–dotted line – $(n,3n)^1$; dashed line – $(n,3n)^2$; full line – $(n,3n)^3$; dashed line – (n,n) + ($n,n\gamma$) for discrete levels; ○ – [13]; ● – [14].

Angular anisotropy of NES of ^{235}U+n interaction observed long ago [13]. The anisotropic contribution of double differential spectra of first neutron, relevant for the excitations of first residual nuclide of 1~6 MeV, is evidenced in double differential NES and mostly in the component of ^{235}U$(n,n\gamma)^1$ reaction. The most investigated to define first neutron spectrum of $(n,nX)^1$ reaction is target nuclide ^{238}U [15]. Emissive neutron spectra of ^{238}U+n interaction are strongly anisotropic. The experimental quasi-differential emissive neutron spectra for ^{235}U+n, ^{238}U+n and ^{239}Pu+n interactions [16, 17] revealed the inadequacy of NES modelling [18, 19] and stimulated further efforts of NES modelling [20].

In the analysis of data on ^{235}U+n interaction the experience obtained in case of ^{238}U+n interaction was employed. Direct excitation of ^{238}U ground state band levels $J^\pi = 0^+, 2^+, 4^+, 6^+, 8^+$ was accomplished within rigid rotator model, while that of β–bands of $K^\pi = 0^+$ and γ–bands of $K^\pi = 2^+$, octupole band of $K^\pi = 0^-$ was accomplished within soft deformable rotator [15, 21, 22] (excitation energies for ^{238}U U=0~1.16 MeV). The net effect of these procedures is the adequate approximation of angular distributions of ^{238}U $(n,nX)^1$ first neutron inelastic scattering in continuum which corresponds to U=1.16~6 MeV excitations for E_n =1.16 MeV~20 MeV. The fictitious levels [19] are avoided, then the approach is applied for the ^{235}U+n interactions to estimate first neutron inelastic scattering in the continuum. The anisotropic part of double differential spectra of first neutron relevant for the excitations of the order of fission barrier value of ^{235}U, will be pronounced in exclusive spectra of $(n,nf)^1$, $(n,2nf)^1$ и $(n,2n)^1$ at E_n >12 MeV [12] which correspond to the various neutron emission angles. Angular distribution of pre-fission

neutrons in [1] was extracted from the observed PFNS of ^{239}Pu(n,F) by subtracting the post-fission neutron spectrum, which was estimated in an approximate manner.

Prompt fission neutron spectra $S(\varepsilon, E_n, \theta)$ at angle θ relative to the incident neutron beam, is a superposition of exclusive spectra of pre-fission neutrons, $(n,nf)^1$, $(n,2nf)^{1,2}$, $(n,3nf)^{1,2,3}$ $-\frac{d^2\sigma^k_{nxn}(\varepsilon, E_n, \theta)}{d\varepsilon d\theta}$ (x=1, 2, 3; k=*1, ...,x*), and spectra of prompt fission neutrons, emitted by fission fragments, $S_{A+1-x}(\varepsilon, E_n, \theta)$:

$$S(\varepsilon, E_n, \theta) = \tilde{S}_{A+1}(\varepsilon, E_n, \theta) + \tilde{S}_{A}(\varepsilon, E_n, \theta) + \tilde{S}_{A-1}(\varepsilon, E_n, \theta) + \tilde{S}_{A-2}(\varepsilon, E_n, \theta) =$$
$$\nu_p^{-1}(E_n, \theta) \cdot \{ \nu_{p1}(E_n) \cdot \beta_1(E_n, \theta) S_{A+1}(\varepsilon, E_n, \theta) + \nu_{p2}(E_n - \langle E_{nnf}(\theta) \rangle) \beta_2(E_n, \theta) S_A(\varepsilon, E_n, \theta) +$$
$$+ \beta_2(E_n, \theta) \frac{d^2\sigma^1_{nnf}(\varepsilon, E_n, \theta)}{d\varepsilon d\varepsilon} + \nu_{p3}(E_n - B_n^A - \langle E^1_{n2nf}(\theta) \rangle - \langle E^2_{n2nf}(\theta) \rangle) \beta_3(E_n, \theta) S_{A-1}(\varepsilon, E_n, \theta) + \beta_3(E_n, \theta) \times$$
$$\left[\frac{d^2\sigma^1_{n2nf}(\varepsilon, E_n, \theta)}{d\varepsilon d\theta} + \frac{d^2\sigma^2_{n2nf}(\varepsilon, E_n, \theta)}{d\varepsilon d\theta} \right] + \nu_{p4}(E_n - B_n^A - B_n^{A-1} - \langle E^1_{n3nf}(\theta) \rangle - \langle E^2_{n3nf}(\theta) \rangle - \langle E^3_{n3nf}(\theta) \rangle) \times$$
$$\beta_4(E_n, \theta) S_{A-2}(\varepsilon, E_n, \theta) + \beta_4(E_n, \theta) \left[\frac{d^2\sigma^1_{n3nf}(\varepsilon, E_n, \theta)}{d\varepsilon d\theta} + \frac{d^2\sigma^2_{n3nf}(\varepsilon, E_n, \theta)}{d\varepsilon d\theta} + \frac{d^2\sigma^3_{n2nf}(\varepsilon, E_n, \theta)}{d\varepsilon d\theta} \right] \}. \quad (1)$$

In equation (1) $\tilde{S}_{A+1-x}(\varepsilon, E_n, \theta)$ is the contribution of x-chance fission to the observed PFNS $S(\varepsilon, E_n, \theta)$, $\langle E^k_{nxnf}(\theta) \rangle$ – average energy of k–th neutron of (n,xnf) reaction with spectrum $\frac{d^2\sigma^k_{nxn}(\varepsilon, E_n, \theta)}{d\varepsilon d\theta}$, $k \le x$. Spectra $S(\varepsilon, E_n, \theta)$, $S_{A+1-x}(\varepsilon, E_n, \theta)$ and $\frac{d^2\sigma^k_{nxn}(\varepsilon, E_n, \theta)}{d\varepsilon d\theta}$ are normalized to unity. Index x denotes the fission chance of $^{236-x}$U after emission of x pre-fission neutrons, $\beta_x(E_n, \theta) = \sigma_{n,xnf}(E_n, \theta) / \sigma_{n,F}(E_n, \theta)$ – contribution of x–th fission chance to the observed fission cross section, $\nu_p(E_n, \theta)$ is the observed average number of prompt fission neutrons, $\nu_{px}(E_{nx})$ – average number of prompt fission neutrons, emitted by $^{236-x}$U nuclides. Spectra of prompt fission neutrons, emitted from fragments, $S_{A+2-x}(\varepsilon, E_n, \theta)$, as proposed in [23], were approximated by the sum of two Watt [24] distributions with different temperatures, the temperature of light fragment being higher.

Modelling the angular distribution for the exclusive spectra of pre-fission neutrons ^{239}Pu(n,xnf)$^{1,\ldots x}$ we reproduced [25] measured data of [1], namely, the ratios of $\langle S(\varepsilon, E_n, \Delta\theta) \rangle_{\Delta E_n} / \langle S(\varepsilon, E_n, \Delta\theta^1) \rangle_{\Delta E_n}$ at $\Delta\theta \sim 35^o$–40^o, $\Delta\theta^1 \approx 130^o - 140^o$ and wide energy range of ΔE_n ~15–17.5 MeV. The ratios of mean energies of PFNS $\langle E(\theta \approx 37.5^o) \rangle / \langle E(\theta^1 \approx 135^o) \rangle$, i.e. of energies $\langle E \rangle$ for neutrons counted at angular intervals $\Delta\theta \sim 35^o$–40^o and $\Delta\theta^1 \sim 130^o$–$150^o$ in E_n~1–20 MeV range. Angular and spin correlations during prompt fission neutron emission are rather tedious, meanwhile the main factor for the observed features of PFNS like ratios for intervals $\langle S(\varepsilon, E_n, \Delta\theta) \rangle_{\Delta E_n} / \langle S(\varepsilon, E_n, \Delta\theta^1) \rangle_{\Delta E_n}$ and $\langle E(\theta \approx 37.5^o) \rangle / \langle E(\theta^1 \approx 135^o) \rangle$, is the excitation energy of fissioning nuclides emerging after x pre-fission neutron emission.

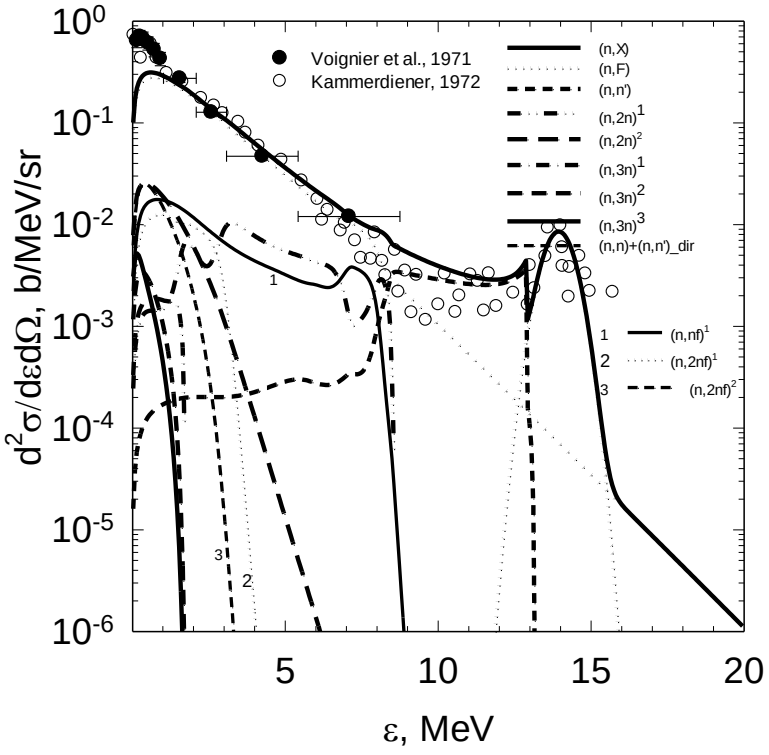

Fig. 2. Double differential neutron emission spectra at E_n =14 MeV, $\theta \approx 30^o$ for ^{235}U(*n,F*) and its partial contributions: full line – (*n,nX*); dotted line – (*n,F*); dashed line – $(n,n\gamma)^1$; dash-double-dotted line – $(n,2n)^1$; dashed line – $(n,2n)^2$; dash-dotted line–$(n,3n)^1$; dashed line – $(n,3n)^2$; full line – $(n,3n)^3$; dashed line – sum of (*n,n*) and $(n,n\gamma)$ for discrete levels;○ – [13]; ● – [14].

Double differential NES could be defined as

$$\frac{d^2\sigma(\varepsilon,E_n,\theta)}{d\varepsilon d\theta}=\frac{1}{2\pi}\Big[\nu_p(E_n,\theta)\sigma_{nF}(E_n,\theta)S(\varepsilon,E_n,\theta)+\sigma_{nn\gamma}(\varepsilon,E_n,\theta)\frac{d^2\sigma^1_{nn\gamma}(\varepsilon,E_n,\theta)}{d\varepsilon d\theta}+$$
$$\sigma_{n2n}(\varepsilon,E_n,\theta)\left(\frac{d^2\sigma^1_{n2n}(\varepsilon,E_n,\theta)}{d\varepsilon d\theta}+\frac{d^2\sigma^2_{n2n}(\varepsilon,E_n,\theta)}{d\varepsilon d\theta}\right)+$$
$$\sigma_{n3n}(\varepsilon,E_n,\theta)\left(\frac{d^2\sigma^1_{n3n}(\varepsilon,E_n,\theta)}{d\varepsilon d\theta}+\frac{d^2\sigma^2_{n3n}(\varepsilon,E_n,\theta)}{d\varepsilon d\theta}+\frac{d^2\sigma^3_{n3n}(\varepsilon,E_n,\theta)}{d\varepsilon d\theta}\right)+$$
$$\sum_q\frac{d\sigma_{nn\gamma}(\varepsilon,E_q,E_n,\theta)}{d\theta}G(\varepsilon,E_q,E_n,\Delta_\theta)\Big], \qquad (2)$$

$$G(\varepsilon,E_q,E_n,\Delta_\theta)=\frac{2}{\Delta_\theta\sqrt{\pi}}\exp\left\{-\left[\frac{\varepsilon-\left(E_n-E_q\right)}{\Delta_\theta}\right]^2\right\}. \qquad (3)$$

NES in Eq. (2) is a superposition of prompt fission neutron spectra $S(\varepsilon,E_n,\theta)$, exclusive spectra of $(n,n\gamma)^1$, $(n,2n)^{1,2}$ и $(n,3n)^{1,2,3}$, $\frac{d^2\sigma^k_{nxn}(\varepsilon,E_n,\theta)}{d\varepsilon d\theta}$, normalized to unity, and spectra of elastic

and inelastic scattered neutrons, followed by excitation of collective levels of ^{235}U, $\frac{d^2\sigma_{nn\gamma}(\varepsilon, E_q, E_n, \theta)}{d\varepsilon d\theta}$. $G(\varepsilon, E_q, E_n, \Delta_\theta)$–resolution function, which depends on E_n and weakly depends on θ. The NES are normalized with average prompt fission neutron number and (*n,xn*) and (*n,F*) cross sections.

The excitation energy of residual nuclides, after emission of (*n,xnf*) neutrons, is decreased by the binding energy of emitted neutron B_{nx} and its average kinetic energy:

$$U_x = E_n + B_n - \sum_{x,1\le k\le x}(< E^k_{nxnf}(\theta) > + B_{nx}). \qquad (4)$$

The excitation energy of fission fragments is

$$E_{nx} = E_r - E^{pre}_{fx} + E_n + B_n - \sum_{x,1\le k\le x}\left(\left\langle E^k_{nxnf}(\theta)\right\rangle + B_{nx}\right). \qquad (5)$$

Value of TKE, kinetic energy of fission fragments prior prompt neutron emission, E^{pre}_F, is approximate by a superposition of partial TKE of $^{240-x}$Pu($^{236-x}$U) nuclides as

$$E^{pre}_F(E_n) = \sum_{x=0}^{X} E^{pre}_{fx}(E_{nx}) \cdot \sigma_{n,xnf} / \sigma_{n,F} \ . \qquad (6)$$

Kinetic energy of fission fragments, i.e. post-fission fragments after neutron emission, E^{post}_F, are defined as

$$E^{post}_F \approx E^{pre}_F\left(1 - \nu_{post}/\left(A + 1 - \nu_{pre}\right)\right). \qquad (7)$$

Similar relation was used for E^{post}_f in [26] at E_n<E_{nnf}. Observed average number of prompt fission neutrons $\nu_p(E_n)$ maybe defined as

$$\nu_p(E_n) = \nu_{post} + \nu_{pre} = \sum_{x=1}^{X} \nu_{px}(E_{nx}) + \sum_{x=1}^{X}(x-1)\cdot\beta_x(E_n). \qquad (8)$$

The post-fission, $\nu_{post}(E_n)$, and pre-fission $\nu_{pre}(E_n)$ partials of $\nu_p(E_n)$ were obtained via consistent description of $\nu_p(E_n)$ and observed fission cross sections at E_n <20 MeV.

Contribution of *x*–th fission chance (*n,xnf*) to the observed fission cross section (*n,F*) is defined as

$$\sigma_{nF}(E_n) = \sigma_{nf}(E_n) + \sum_{x=1}^{X}\sigma_{n,xnf}(E_n) \ . \qquad (9)$$

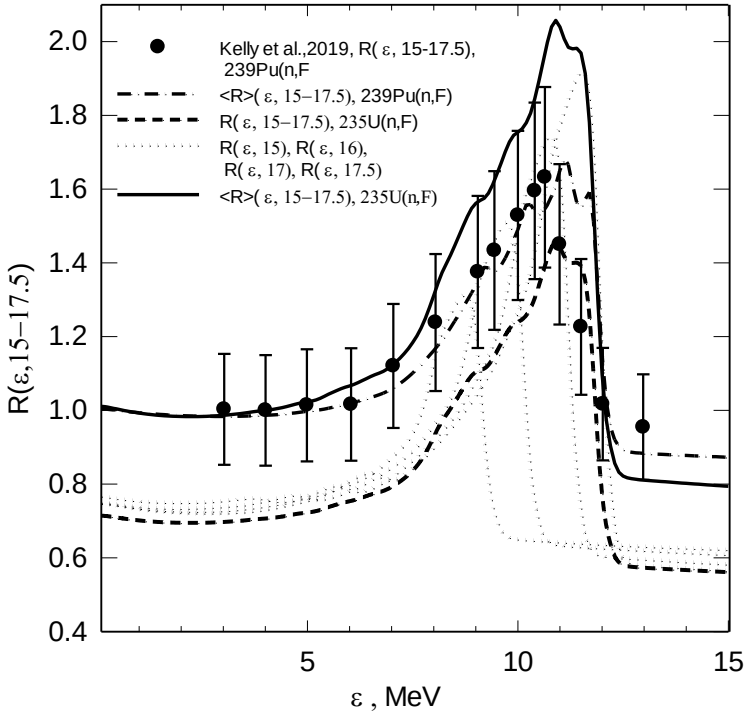

Fig. 3 Measured ratio $R^{\exp} = S(\varepsilon, E_n \approx 15-17.5, \Delta\theta)/S(\varepsilon, E_n \approx 15-17.5, \Delta\theta^1)$ of ^{235}U(*n,F*) PFNS and calculated $R(\varepsilon,15\div17.5)$ for "forward", $\Delta\theta$ ~35°–40°, and "backward" emission, $\Delta\theta^1$=130°–140°; ●–^{239}Pu(*n,F*) [1]; full line – ^{235}U(*n,F*) PFNS normalized to unity; dashed line – ^{235}U(*n,F*) PFNS equated at ε~3–5 MeV; dash-dotted line – ^{239}Pu(*n,F*) PFNS equated at ε~3–5 MeV; dotted line – partials of ^{235}U(*n,F*) $R(\varepsilon,15\div17.5)$ at E_n ~ 15 MeV, E_n ~ 16 MeV, E_n ~ 17 MeV and E_n ~ 17.5 MeV.

That means the (*n,xnf*) contributions are defined by the fission probability $P^{J\pi}_{f(A+1-x)}(E)$ of $^{236\text{-}x}$U nuclides:

$$\sigma_{n,xnf}(E_n) = \sum_{J\pi}^{J} \int_0^{U_x} W^{J\pi}_{A+1-x}(U) P^{J\pi}_{f(A+1-x)}(U) dU\,, \qquad (10)$$

here $W^{J\pi}_{A+1-x}(U)$ is the population of excited states of (*A+1–x*) nuclides with excitation energy *U* after emission of *x* post-fission neutrons.

The QRPA methods are the most advanced, however they are still incapable to describe NES of ^{238}U+*n* [18]. Emission spectrum of $(n,nX)^1$ reaction, $\frac{d^2\sigma^1_{nnx}(\varepsilon, E_n, \theta)}{d\varepsilon d\theta}$, could be represented by the sum of compound and weakly dependent on emission angle pre-equilibrium components, and phenomenological function, modelling energy and angle dependence of NES [13] with first neutron inelastic scattering in continuum [1, 12, 27, 28]:

$$\frac{d^2\sigma^1_{nnx}(\varepsilon, E_n, \theta)}{d\varepsilon d\theta} \approx \frac{d^2\tilde{\sigma}^1_{nnx}(\varepsilon, E_n, \theta)}{d\varepsilon d\theta} + \sqrt{\frac{\varepsilon}{E_n}} \frac{\omega(\theta)}{E_n - \varepsilon} \qquad (11)$$

$$\omega(\theta) = 0.4\cos^3(\theta) + 0.16 \qquad (12)$$

Angle-averaged function $\omega(\theta)$ [28], $\langle\omega(\theta)\rangle_\theta$ for angles $\theta_2-\theta_1=135^o-30^o$ [1], is approximated as $\langle\omega(\theta)\rangle_\theta\approx\omega(90^o)$, then angle-integrated spectrum equals

$$\frac{d\sigma^1_{nnx}(\varepsilon,E_n)}{d\varepsilon}\approx\frac{d\tilde{\sigma}^1_{nnx}(\varepsilon,E_n)}{d\varepsilon}+\sqrt{\frac{\varepsilon}{E_n}}\frac{\langle\omega(\theta)\rangle_\theta}{E_n-\varepsilon}. \quad (13)$$

To retain the flux conservation in cross section and spectra calculations the compound reaction cross sections in [28] renormalized to account for extra semidirect neutron emission:

$$\sigma_c(E_n)=\sigma_a(E_n)(1-q-\tilde{q}), \quad (14)$$

Emission spectrum of $(n,nX)^1$, q–ratio of pre-equilibrium neutrons in a standard pre-equilibrium model [29],

$$\frac{d\tilde{\sigma}^1_{nnx}(\varepsilon,E_n)}{d\varepsilon}=\sum_{J,\pi}W_A^{J\pi}(E_n-\varepsilon,\theta), \quad (15)$$

depends on fission probability of $(A+1)$ nuclide. It defines the exclusive spectra of each partial reaction in STAPRE [29] framework, $W_A^{J\pi}(E_n-\varepsilon,\theta)$ is the population of residual nuclide A states with spin/parity J^π and excitation energy $U=E_n-\varepsilon$, after first neutron emission at angle θ. Henceforth the indexes J^π in fission, Γ_f, neutron Γ_n and total Γ widths described in [30], as well as relevant summations, omitted. The angular dependence of partial width, calculated with spin and parity conservation, is due to dependence of excitation energy of residual nuclides on the emission angle of first neutron. The exclusive spectra of pre-fission $(n,nf)^1$ neutron is

$$\frac{d^2\sigma^1_{nnf}(\varepsilon,E_n,\theta)}{d\varepsilon d\theta}=\frac{d^2\sigma^1_{nnx}(\varepsilon,E_n,\theta)}{d\varepsilon d\theta}\frac{\Gamma_f^A(E_n-\varepsilon,\theta)}{\Gamma^A(E_n-\varepsilon,\theta)}. \quad (16)$$

First neutron spectra of $(n,2nf)^1$ for reaction $(n,2nf)$, is defined as:

$$\frac{d^2\sigma^1_{n2nf}(\varepsilon,E_n,\theta)}{d\varepsilon d\theta}=\int_0^{E-B_n^A}\frac{d^2\sigma^1_{n2nx}(\varepsilon,E_n,\theta)}{d\varepsilon d\theta}\frac{\Gamma_f^{A-1}(E_n-B_n^A-\varepsilon-\varepsilon_1)}{\Gamma^{A-1}(E_n-B_n^A-\varepsilon-\varepsilon_1)}d\varepsilon_1, \quad (17)$$

here first neutron spectra of $(n,2nx)$ reaction, i.e. $(n,2nx)^1$, is defined by the neutron spectrum of $(n,nX)^1$ and neutron emission probability of nuclide A as:

$$\frac{d^2\sigma^1_{n2nx}(\varepsilon,E_n,\theta)}{d\varepsilon d\theta}=\frac{d^2\sigma^1_{nnx}(\varepsilon,E_n,\theta)}{d\varepsilon d\theta}\frac{\Gamma_n^A(E_n-\varepsilon,\theta)}{\Gamma^A(E_n-\varepsilon,\theta)}. \quad (18)$$

Spectra of first and next neutrons of ^{238}U(*n,3nf*) reaction are covered in [6], in case of ^{235}U(*n,3nf*) reactions they are defined in a similar fashion, but their contribution is quite low, actually less than ~10-20 mb.

Phenomenological approach enables to reproduce NES in case of ^{235}U+n interactions. Fig. 1 and Fig. 2 show comparisons of calculated double differential NES of ^{235}U +*n*, at E_n~14 MeV, θ~30º and θ~135º with measured data [13, 14]. Exclusive pre-fission neutron spectra of ^{235}U$(n,xnf)^{1,2}$ are shown on Fig. 1 and Fig. 2 as $\frac{\sigma_{n,xnf}(E_n,\theta)}{4\pi}\frac{d\sigma^{1,2}_{nnf}(\varepsilon,E_n,\theta)}{d\varepsilon}$ at angles θ~30º and θ~135º. They comprise small part of $(n,nX)^1$ spectrum, nonetheless they reproduce angular dependence of PFNS with respect to the incident neutron beam.

Angular distributions of ^{239}Pu(*n,xnf*) pre-fission neutrons at E_n ~14–18 MeV, measured in [1], may be quite well described as $0.25\,\omega(\theta)$, if θ>135º, then $0.25\,\omega(\theta=135^o)$. Estimate of pre-fission neutrons contribution in [1] at any E_n or θ, was obtained as difference of observed PFNS and some simple estimate of post-fission neutrons evaporated from fission fragments. Though the procedure adopted in [1] is susceptible to systematic uncertainties, since post-fission neutrons may emerge from (*x*+1) fissioning nuclides [6–12], it seems hidden normalizations were used in [1]. It seems the normalization in [1] was accomplished in the energy range $\varepsilon>E_{nnf1}$, here E_{nnf1} is the upper energy of exclusive neutron spectra of $(n,nf)^1$ neutrons.

Angular anisotropy of PFNS relative to incident neutron beam was detected in ^{239}Pu(*n,F*) [1] at E_n~15–17.5 MeV range and at $\Delta\theta$ ~35º–40º (forward direction) and $\Delta\theta^1$=130º–140º (backward direction). The data normalization obtained by equating PFNS at ε~3–5 MeV energy range. Alternative representation of PFNS, against that shown on Fig.3 in [1], as a ratio $R^{\exp}=S(\varepsilon,E_n\approx15-17.5,\Delta\theta)/S(\varepsilon,E_n\approx15-17.5,\Delta\theta^1)$ for $\Delta\theta$ ~35º–40º (forward direction) and $\Delta\theta^1$=130º–140º (backward direction) is virtually independent upon the normalizations adopted in [1].

Fig. 3 shows $R^{\exp}$ of ^{239}Pu(*n,F*) ratio $R^{\exp}$ of PFNS and calculated ratio of ^{235}U(*n,F*) at E_n~15–17.5 MeV $\Delta\theta$ ~35º–40º (forward direction) and $\Delta\theta^1$=130º–140º (backward direction) are compared with calculated ratio

$$R(\varepsilon,15\div17.5)\approx\frac{\int_{15}^{17.5}\nu_p(E_n,\approx30^o)\sigma_{nF}(E_n,\approx30^o)S(\varepsilon,E_n,\theta\approx30^o)\varphi(E_n)dE_n}{\int_{15}^{17.5}\nu_p(E_n,\theta\approx135^o)\sigma_{nF}(E_n,\theta\approx135^o)S(\varepsilon,E_n,\theta\approx135^o)\varphi(E_n)dE_n},\qquad(19)$$

here $\varphi(E_n)$ is the incident neutron spectrum, which is unknown. Spectra $S(\varepsilon,E_n,\theta)$ normalized to unity. As a first order approximation $R(\varepsilon,15\div17.5)$ might be calculated as a ratio of $\nu_p(E_n,\theta)\sigma_{nF}(E_n,\theta)S(\varepsilon,E_n\approx15-17.5,\Delta\theta)/\nu_p(E_n,\theta)\sigma_{nF}(E_n,\theta)S(\varepsilon,E_n\approx15-17.5,\Delta\theta^1)$ for E_n ~ 15 MeV, E_n ~ 16 MeV, E_n ~ 17 MeV and E_n ~ 17.5 MeV. Values of $\nu_p(E_n,\theta)$ and $\sigma_{nF}(E_n,\theta)$ were calculated at the same energies E_n, as those in $S(\varepsilon,E_n\approx15-17.5,\Delta\theta)$. In case of angular dependent observables for ^{235}U(*n,F*) hidden structures in lumped $R(\varepsilon,15\div17.5)$ constituents (for monochromatic beams) are smoothed, then $R^{\exp}$ and $R(\varepsilon,15-17.5)$ seem to have similar shapes,

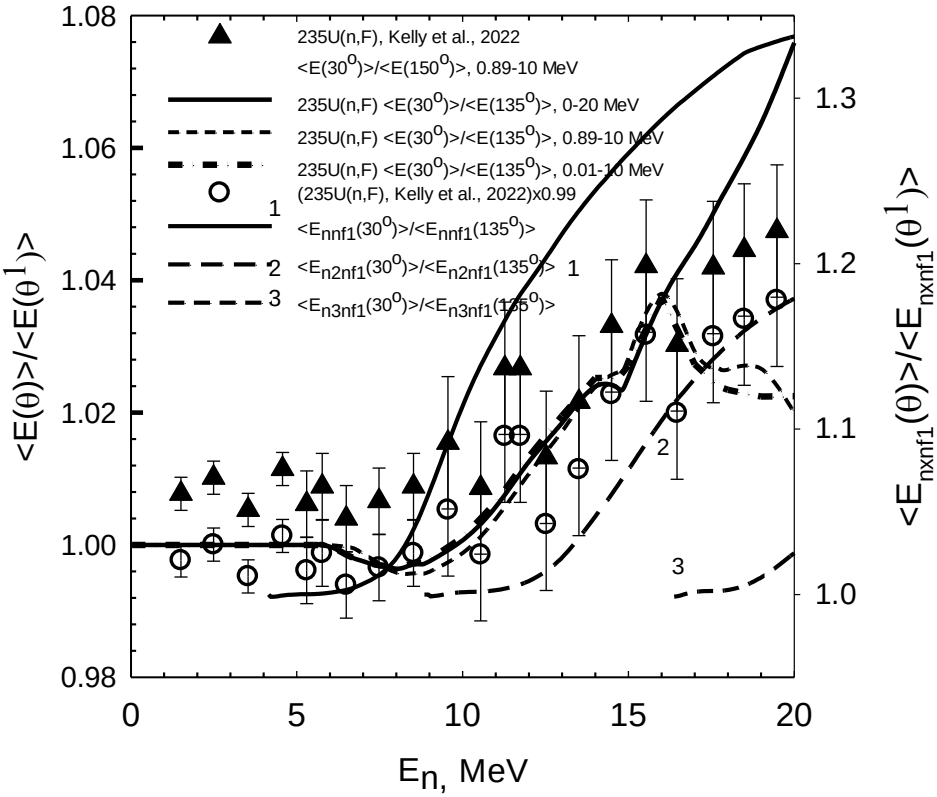

Fig. 4. Ratio $\langle E(\theta)\rangle/\langle E(\theta^1)\rangle$ for ^{235}U(n,F) PFNS: ▲– $\langle E(\theta\approx 30^o)\rangle/\langle E(\theta^1\approx 135^o)\rangle$, ε~1–12 MeV [4]; ○–$\langle E(\theta\approx 30^o)\rangle/\langle E(\theta^1\approx 135^o)\rangle\times 0.99$, [4]; full line–$\langle E(\theta\approx 30^o)\rangle/\langle E(\theta^1\approx 135^o)\rangle$, ε~1–20 MeV; dashed line–$\langle E(\theta\approx 30^o)\rangle/\langle E(\theta^1\approx 135^o)\rangle$, ε~0.89–10 MeV; dash–dotted line – $\langle E(\theta\approx 30^o)\rangle/\langle E(\theta^1\approx 135^o)\rangle$, ε~0.01–10 MeV; dash–dotted line –$\langle E(60^o)/E(90^o)\rangle$, ε~0–20 MeV; lines 1, 2, 3 –$\langle E_{n,xnf}(\theta\approx 30^o)\rangle/\langle E_{n,xnf}(\theta^1\approx 135^o)\rangle$, x=1, 2, 3.

but the latter is shifted downwards. Smooth line of $R(\varepsilon,15-17.5)$ at Fig. 3 obtained by assuming in equation (20) equality of numerator and denominator values at ε~3–5 MeV energy range, as adopted in [1]. In case of ^{235}U(n,F) and ^{239}Pu(n,F) at $\varepsilon>E_{nnf1,}$ both $R^{\exp}$ and $R(\varepsilon,15-17.5)$ are less then unity, that might be due to influence of angular dependence of (n,xnf) neutron emission on the fission chances distribution. The renormalized $R(\varepsilon,15-17.5)$ seems to be consistent with $R^{\exp}$ data.

The calculated anisotropy of pre-fission neutrons of ^{235}U(n,xnf) reaction is a bit higher than in case of ^{239}Pu(n,F). That might be due to correlation of anisotropy of pre-fission neutrons with contribution of emissive fission (n,nf) to the observed fission cross section, PFNS and angular anisotropy of NES. In case of ^{235}U(n,F) and ^{239}Pu(n,F) at $\varepsilon>E_{nnf1,}$ both $R^{\exp}$ and $R(\varepsilon,15-17.5)$ are less then unity, that also might be due to influence of angular dependence of (n,xnf) neutron emission on the fission chances distribution.

Angular dependence of the first pre-fission neutron in reactions (n,nf)^1 and (n,$2nf$)^1 [25] allows to interpret the experimental data trend in case of ratio of average energies for “forward”

and "backward" emission of pre-fission neutrons in ^{239}Pu(n,xnf)^{1,2,3} [1] and ^{235}U(n,xnf)^{1,2,3} [4] reactions. The ratio of $\langle E(\theta)\rangle/\langle E(\theta^1)\rangle$ [1] in case of ^{239}Pu(n,F) for "forward", $\Delta\theta$ ~35^o–40^o, and "backward", $\Delta\theta^1$=130^o–140^o, emission of pre-fission neutrons steeply increases starting from E_n~10–12 MeV. Pre-fission (n,nf)^1 neutrons are responsible for that. The angular anisotropy of (n,xnf)^1 neutrons emission is due to pre-equilibrium/semidirect emission of first neutron in (n,nX)^1. When average energies are calculated at energy range of ε~1–3 MeV, ratios $\langle E(\theta)\rangle/\langle E(\theta^1)\rangle$ are virtually independent on E_n, while the dependence of ratio $\langle E(60^o)\rangle/\langle E(90^o)\rangle$ upon E_n, when averaging is for ε~1–12 MeV, is rather weak [25].

The ratio of average energies of exclusive neutron spectra of ^{235}U(n,nf)^1, $\frac{d^2\sigma^1_{nnf}(\varepsilon,E_n,\theta\approx 30^o)}{d\varepsilon d\theta}$ and $\frac{d^2\sigma^1_{nnf}(\varepsilon,E_n,\theta\approx 135^o)}{d\varepsilon d\theta}$, $\langle E_{n,xnf}(\theta\approx 30^o)\rangle/\langle E_{n,xnf}(\theta^1\approx 135^o)\rangle$, is much higher than that of $\langle E(\theta)\rangle/\langle E(\theta^1)\rangle$, however it follows the shape of experimental ratio $\langle E(\theta\approx 30^o)\rangle/\langle E(\theta^1\approx 135^o)\rangle$ [1, 4]. Angular dependence of the ratio of average energies of exclusive neutron spectra of ^{235}U($n,2nf$)^1 $\frac{d^2\sigma^1_{n2nf}(\varepsilon,E_n,\theta\approx 30^o)}{d\varepsilon d\theta}$ and $\frac{d^2\sigma^1_{n2nf}(\varepsilon,E_n,\theta\approx 150^o)}{d\varepsilon d\theta}$ is much weaker. In the ratio of average energies of exclusive neutron spectra of ^{235}U($n,3nf$)^1, $\frac{d^2\sigma^1_{n3nf}(\varepsilon,E_n,\theta\approx 30^o)}{d\varepsilon d\theta}$ and $\frac{d^2\sigma^1_{n3nf}(\varepsilon,E_n,\theta\approx 150^o)}{d\varepsilon d\theta}$, the angular dependence is quite weak. Ratios $\langle E(\theta\approx 30^o)\rangle/\langle E(\theta^1\approx 135^o)\rangle$ are virtually independent upon the lower threshold of neutron detection, while the dependence upon angular range and value of higher neutron detection threshold (ε~12 or ε~20 MeV) is crucial. That is illustrated on Fig. 4 for ratios of $\langle E(\theta\approx 30^o)\rangle/\langle E(\theta^1\approx 135^o)\rangle$ and $\langle E(\theta\approx 60^o)\rangle/\langle E(\theta^1\approx 90^o)\rangle$.

Calculated ratio $\langle E(\theta\approx 30^o)\rangle/\langle E(\theta^1\approx 135^o)\rangle$ for ^{235}U(n,F) PFNS is also somewhat higher than in case of ^{239}Pu(n,F) PFNS [25, 28], which seems to be compatible with higher contribution of ^{235}U(n,nf) reaction to the observed fission cross section ^{235}U(n,F). For emitted neutrons energy range of ε~1–12 MeV or ε~0–20 MeV, as evidenced on Fig. 4, $\langle E(\theta\approx 30^o)\rangle/\langle E(\theta^1\approx 135^o)\rangle$ is quite consistent with measured data for ^{235}U(n,F) up to E_n ~16 MeV. Calculated ratios $\langle E(\theta\approx 30^o)\rangle/\langle E(\theta^1\approx 135^o)\rangle$ for ε~0–20 MeV are much higher than measured data for ε~1–12 MeV. Data of [4] for ^{235}U(n,F) were multiplied by 0.99 factor to attain visible consistency of measured and calculated data $\langle E(\theta\approx 30^o)\rangle/\langle E(\theta^1\approx 135^o)\rangle$. For exclusive neutron spectra of ^{235}U(n,nf)^1 the ratios of $\frac{d^2\sigma^1_{nnf}(\varepsilon,E_n,\theta\approx 30^o)}{d\varepsilon d\theta}$ and $\frac{d^2\sigma^1_{nnf}(\varepsilon,E_n,\theta\approx 135^o)}{d\varepsilon d\theta}$ average energies are also much higher than those of $\langle E(\theta)\rangle/\langle E(\theta^1)\rangle$, but their shape is virtually consistent with that of $\langle E(\theta\approx 30^o)\rangle/\langle E(\theta^1\approx 135^o)\rangle$ [4] (see Fig. 4).

Average energy $\langle E\rangle$ is a rough integral estimate of PFNS, however the angular anisotropy of pre-fission neutron emission exerts quite an influence on it. Dependence of $\langle E\rangle(E_n)$ in case of ^{235}U(n,F) is compared with measured data for energy range ε~0.01 – 10 MeV [2, 3] on Fig. 5.

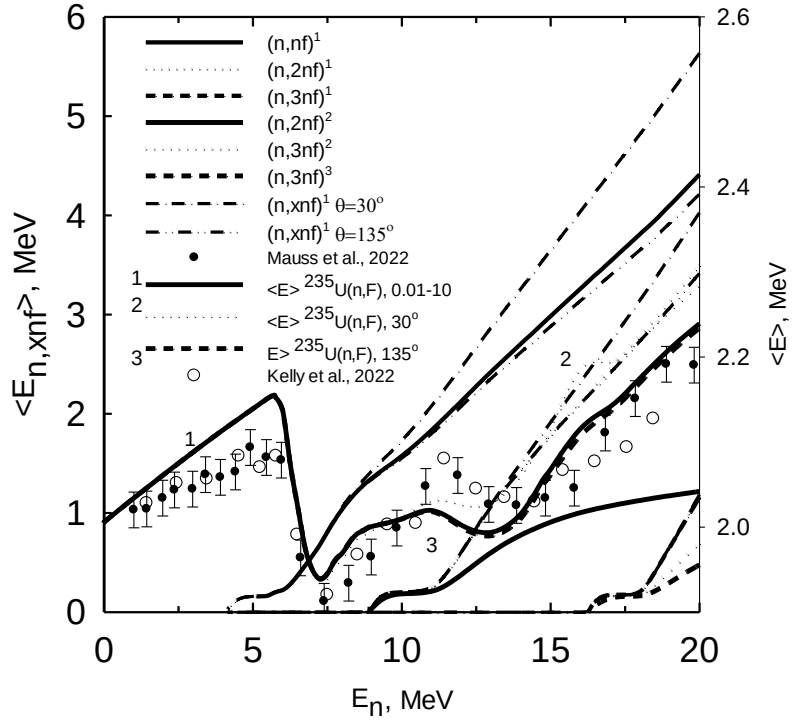

Fig. 5 PFNS $\langle E \rangle$ for ^{235}U(*n, F*): ○–[4]; ● –[5]; full line, 1 –$\langle E(90^o) \rangle$; dotted line, 2 – $\langle E(30^o) \rangle$; dashed line, 3–$\langle E(135^o) \rangle$; full line – $\langle E_{n,xnf}(\theta \approx 90^o) \rangle$; dash–dotted line–$\langle E_{n,xnf}(\theta \approx 30^o) \rangle$; dash–double dotted line–$\langle E_{n,xnf}(\theta \approx 135^o) \rangle$.

The estimates of $\langle E \rangle$ for PFNS of ^{235}U(*n,F*) are strongly correlated with PFNS influence of exclusive neutron spectra of (*n,nf*)^{1} and (*n,2nf*)^{1,2} which they exert on $\langle E \rangle$ in case of ^{235}U(*n,F*) are much stronger than in case of ^{239}Pu(*n,F*). There still are some minor discrepancies between measured and calculated $\langle E \rangle$, that might be due to arbitrary normalizations when two neutron detectors are used in [1, 3, 4] at ε<1.5 MeV and ε>0.8 MeV. Mutual normalization in these two overlapping energy ranges is susceptible uncertainty of detector efficiency and data scatter.

Analysis of prompt fission neutron spectra of ^{235}U(*n,F*) evidenced correlations of a number observed data structures with (*n,xnf*)$^{1\ldots x}$ pre-fission neutrons. Pre-fission neutron spectra turned out to be quite soft as compared with neutrons emitted by excited fission fragments. The net outcome of that is the decrease of $\langle E \rangle$ in the vicinity of the (*n,xnf*) thresholds of ^{235}U(*n,F*). The amplitude of the $\langle E \rangle$ variation is much higher in case of ^{235}U(*n,F*) as compared with ^{239}Pu(*n,F*). The correlation of PFNS shape with different angles of emission of (*n,xnf*)^{1} neutrons and emissive fission contributions for ^{235}U(*n,F*) is established. The angular anisotropy of exclusive pre-fission neutron spectra strongly influences the PFNS shapes and $\langle E \rangle$. These peculiarities are due to differing emissive fission contributions in ^{239}Pu(*n,F*) and ^{235}U(*n,F*) [31, 32]. Calculated ratio of $\langle E \rangle$ for "forward" and "backward" emission of pre-fission neutrons steeply increases with the increase of average energies of exclusive pre-fission neutron spectra.

References

1. K. J. Kelly, T. Kawano, J.M. O'Donnel et al., Phys. Rev. Lett., 122, 072503 (2019).
2. P. Marini, J. Taieb, B. Laurent et al., Phys. Rev. C, 101, 044614 (2020).
3. K. J. Kelly, M. Devlin, O'Donnel J.M. et al., Phys. Rev. C, 102, 034615 (2020).
4. K. J. Kelly, J.A. Gomez, M. Devlin et al., Phys. Rev. C, 105, 044615 (2022).
5. B. Mauss, J. Taieb, B. Laurent et al., https://oecd-nea.org/dbdata/nds_jefdoc/jefdoc-2200.pdf, Nuclear Data Week, November, 2022, JEFDOC-2200.
6. V.M. Maslov, Yu. V. Porodzinskij, M. Baba, A. Hasegawa, N.V. Kornilov, A.B. Kagalenko and N.A. Tetereva, Phys. Rev. C, 69, 034607 (2004).
7. V.M. Maslov, N.V. Kornilov, A.B. Kagalenko and N.A. Tetereva, Nucl. Phys. A, 760, 274 (2005), https://www–nds.iaea.org/ minskact/ data/ 92235f18.txt.
8. V.M. Maslov, At. Energy, 103, 119 (2007).
9. V.M. Maslov, V.G. Pronyaev, N.A. Tetereva et al., At. Energy, 108, 352 (2010).
10. V.M. Maslov,V.G. Pronyaev, N.A. Tetereva et al., J. Kor. Phys. Soc. 59, 1337 (2011).
11. V.M. Maslov, Yad. Fiz., 71, 11 (2008)
12. V.M. Maslov In: Proc. LXXII Intern. Conf. Nucleus 2022, Fundamental problems and applications, Moscow, 11–16 July, 2022, Book of abstracts, p. 111, https:// events . sinp.msu.ru/event/8/attachments/181/875 nucleus–2022–book–of–abstracts–www.pdf.
13. J.L. Kammerdiener, UCRL–51232, 1972.
14. J. Voignier, R.G. Clayeux, F. Bertrand, CEA-R-3936, 1970.
15. V.M. Maslov, M. Baba, A. Hasegawa, A. B Kagalenko., N.V. Kornilov, N.A. Tetereva, INDC (BLR)-14, Vienna: IAEA, 2003; https://www-nds.iaea.org/publications/ indc/indc-blr-0014/.
16. A.M. Daskalakis, R.M.Bahran, E.J. Blain et al., Ann. Nucl. Energy, 73, 455 (2014).
17. K. S. Mohindroo, Y. Danon, E.J. Blain et al., Ann. Nucl. Energy, 165, 108647 (2022).
18. M. Dupuis, S. Hilaire, S. Peru, EPJ Web of Conferences, 146, 12002 (2017).
19. P. Young, M. Chadwick, R. MacFarlane et al., Nucl. Data Sheets, 108, 2589 (2007).
20. M. R. Mumpower, D. Neudecker, H. Sasaki, et al., Phys. Rev. C, 107, 034606 (2023).
21. V.M. Maslov, Yu.V. Porodzinskij, M. Baba, A. Hasegawa, Bull. RAS, Ser. Fyz. 67, 1597 (2003).
22. V.M. Maslov, Yu.V. Porodzinskij, N.A. Tetereva et al., Nucl. Phys. A, 2006, 764, 212.
23. N.V. Kornilov, A.B. Kagalenko, F.-J. Hambsch, Yad. Fiz. 62, 209 (1999).
24. B.E. Watt, Phys. Rev., 87, 1037, (1952)
25. V.M. Maslov, Proc. 28th International Seminar on Interactions of Neutrons with Nuclei, 2021, May, 24-28, Dubna, Russia, Book of Abstracts, p. 113, http://isinn.jinr.ru/past-isinns/isinn 28/ISINN 28 %20 Abstract%20 Book.pdf.
26. D.G. Madland, A.C. Kahler, Nucl. Phys. A 957, 289 (2017).
27. V.M. Maslov, in: Proc. LXXII Intern. Conf. Nucleus 2022, Fundamental problems and applications, Moscow, 11–16 July, 2022, p. 168. https://events.sinp.msu.ru/event/ 8/contributions/ 586/attachments/568/881/mvmNucl 2022%2 B.pdf
28. V.M. Maslov, Physics of Particles and Nuclei Letters, 20, 1401 (2023).
29. M. Uhl and B. Strohmaier, IRK-76/01, IRK, Vienna, 1976.
30. V.M. Maslov, Phys. Rev. C, 72, 044607 (2005).
31. V.M. Maslov, Physics of Particles and Nuclei Letters, 20, 565 (2023).
32. V.M. Maslov, Yad. Fyz., 86, 562 (2023).